Power output fluctuations in large scale PV plants: one year observations with one second resolution and a derived analytic model

Javier Marcos[1*], Luis Marroyo[1], Eduardo Lorenzo[2], David Alvira[3] and Eloisa Izco[4]

[1] Dpto. Ingeniería Eléctrica y Electrónica, Universidad Pública de Navarra, Campus Arrosadia, 31006 Pamplona, Spain
[2] Instituto de Energía Solar, ETSI Telecomunicación, Ciudad Universitaria, s/n, 28040, Madrid, Spain
[3] Red Eléctrica de España, C/Anabel Segura 11, 28108 Alcobendas, Spain
[4] Acciona Solar, Avda. de la Ciudad de la Innovación, 3, 31621 Sarriguren, Navarra, Spain

ABSTRACT

The variable nature of the irradiance can produce significant fluctuations in the power generated by large grid-connected photovoltaic (PV) plants. Experimental 1 s data were collected throughout a year from six PV plants, 18 MWp in total. Then, the dependence of short (below 10 min) power fluctuation on PV plant size has been investigated. The analysis focuses on the study of fluctuation frequency as well as the maximum fluctuation value registered. An analytic model able to describe the frequency of a given fluctuation for a certain day is proposed.

KEYWORDS

large PV plants; grid-connected; power fluctuations; analytic model

***Correspondence**

Javier Marcos, Edificio Los Pinos, Dpto. Ingeniería Eléctrica y Electrónica, Universidad Pública de Navarra, Campus Arrosadia, 31006 Pamplona, Spain.
E-mail: javier.marcos@unavarra.es

1. INTRODUCTION

The power generated by photovoltaic (PV) plants has a variable character mainly due to the changeability of cloudiness. As penetration of PV energy in the grid increases, such variability can negatively affect power quality and reliability. Nowadays this issue is of special importance in small grids (like islands) with high PV penetration. Thus, the research interest in PV power fluctuations. Irradiance fluctuations have been observed and analysed at Germany [1,4] Japan [2], Belgium [3] and Australia [4] USA [8–13]. However, power output fluctuations analyses are significantly scarce. The available experimental data consist of a 1 year 5 min data from 100 PV sites (totalling 243 kWp) in Germany [5]; 10 s and 1 min data from a single 4.6 MWp PV site and 10 min data from three ~100 kW sites in Arizona (USA) [6] and 3 month 1 min data from 52 PV sites of an average of 3.2 kWp, in Japan [7].

In this paper, 1 year 1 s data from six PV plants in Spain, ranging from 1 to 9.5 MWp totalling 18 MWp, has been considered. In addition to this, data from two sections (correspondingly, 48 and 143 kWp) of a PV plant have also been registered. Particular attention has been paid to the analysis of the influence on the magnitude of the power fluctuations of both, the size of the PV plant and the sampling period. An analytical model to describe the daily frequency of undergoing a power fluctuation of a certain magnitude is presented. Further studies to assess the geographic smoothing are currently undertaken and will be reported in the near future.

2. EXPERIMENTAL SET-UP

Figure 1 and Table I detail the location of the six sites considered, and the power and extension of the PV plants. The plants under analysis are scattered over a ~1000 km^2 area in the south of Navarra (Spain). The distancing between the plants ranges from 6 to 60 km. All the PV plants are equipped with vertical axis trackers, and feed power to the 13.2 kV grid. Table I also shows the short-circuit power of the grid at the point of common coupling for each installation.

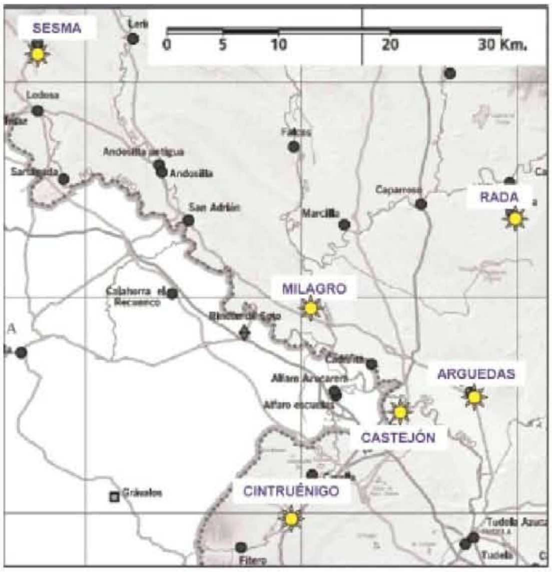

Figure 1. Location of the 6 PV plants under study

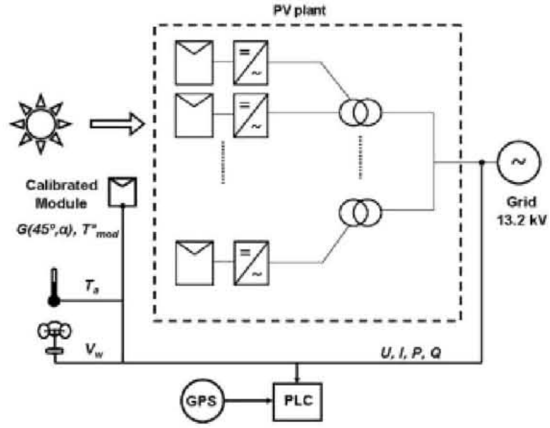

Figure 2. Diagram of the experimental set-up

Figure 2 shows the experimental set-up installed at the PV plants. Power output 1 s data are obtained at the point of common coupling by means of a power meter (Allen-Bradley, Powermonitor), and are recorded by a PLC (Allen-Bradley, CompactLogix). Simultaneously, the short circuit current of a reference PV module provide a measurement of in-plane irradiance, which is also recorded. Wind speed (at 2 m high), ambient temperature and cell temperature are registered too. Timing is controlled by means of a GPS so that the records from all the sites can be precisely synchronized. Data recording started on April 17th, 2008 and is still undergoing. Current rough data is over 45 GB.

As an example, Figure 3 shows the irradiance, G (W/m^2) and the output power (normalized and scaled by a factor of 1000, P_N) recorded at Milagro 9.5 MWp site, on August 12th, from 13:07 to 13:20 h. Because of the big size of the PV plant, the power curve is significantly smoother than the irradiance.

3. DEFINITIONS

The magnitude of a power fluctuation $\Delta P_{\Delta t}(t)$ at an instant t for a given sampling period, Δt, is calculated as the difference between the two power outputs, normalized to the transformer power P^* of the plant under consideration, Equation (1). That is:

$$\Delta P_{\Delta t}(t) = \frac{[P(t+\Delta t) - P(t)]}{P^*} \quad (1)$$

This definition can also be applied to irradiance fluctuations, $\Delta G_{\Delta t}$, normalizing by $G^* = 1000\,\text{W/m}^2$.

Now, let us consider a time series of power outputs. The fluctuations during a certain elapsed time might be observed by going over the series with a Δt wide time window. This window has the same time step that the raw data resolution (1 s). This way, a time series of power fluctuation is derived from a time series of power output for a given Δt. Note that Δt can be any multiple of the raw data resolution. Figure 4 shows the fluctuation evolution corresponding to the irradiance (ΔG) and the output power (ΔP) of Figure 3, for $\Delta t = 10$ and 60 s. The smoothing from irradiance to power is clearly observed in both Δt cases. As expected, the larger the sampling-time, the larger the fluctuations.

Strictly speaking, the magnitude of a fluctuation $\Delta P_{\Delta t}(t)$ at an instant t for a given Δt must be calculated as the difference between the maximum and the minimum values observed all over Δt, that is:

$$\Delta P_{\Delta t}(t) = \frac{\max[P(t, t+\Delta t)] - \min[P(t, t+\Delta t)]}{P^*} \quad (2)$$

It can be argued that results given by Equation (1) do not properly represent the real fluctuation because aliasing can occur, particularly for relatively large values of Δt. However,

Table I. PV plants characteristics

PV plants	Peak power (kWp)	Rated power (kW)	Area (Ha)	Grid short-circuit power (MVA)	Location (Lat; Lon)
Arguedas	958	775	4.1	38.8	42°10′32″ N 1°35′28″ W
Sesma	990	800	4.2	43.4	42°27′43″ N 2° 5′31″ W
Cintruénigo	1438	1155	6.4	41.2	42° 3′35″ N 1°47′50″ W
Rada	1780	1400	8.7	36.6	42°19′3.25″ N 1°34′10″ W
Castejón	2640	2000	11.8	38.9	42° 9′7″ N 1°39′36″ W
Milagro	9500	7243	52	49.7	42°15′28.24″ N 1°46′30″ W
Milagro section 1	48	35	0.21	—	42°15′28.24″ N 1°46′30″ W
Milagro section 2	143	100	0.63	—	42°15′28.24″ N 1°46′30″ W

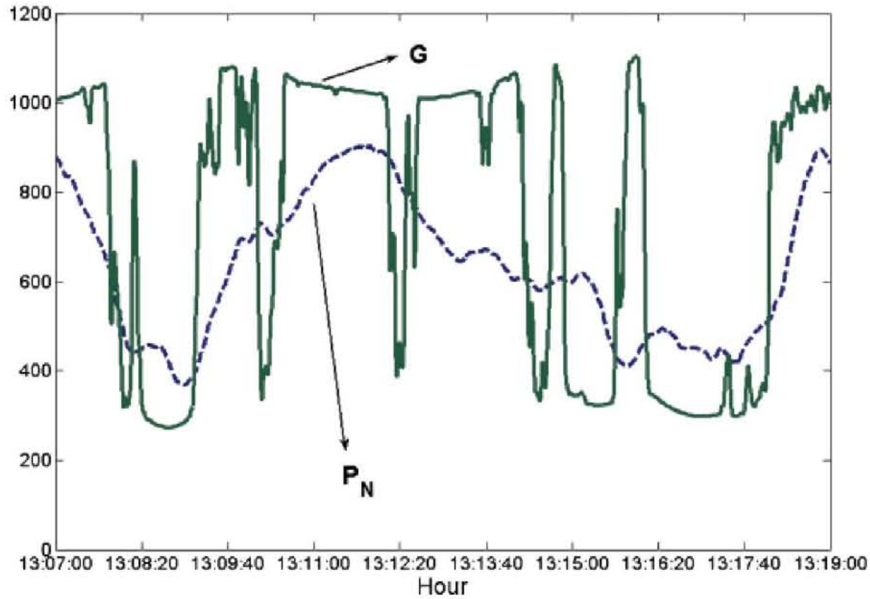

Figure 3. Irradiance, G (W/m^2), and output power P_N(normalized and scaled by a factor of 1000) recorded at Milagro site during a 15-min period on 12/8/2008

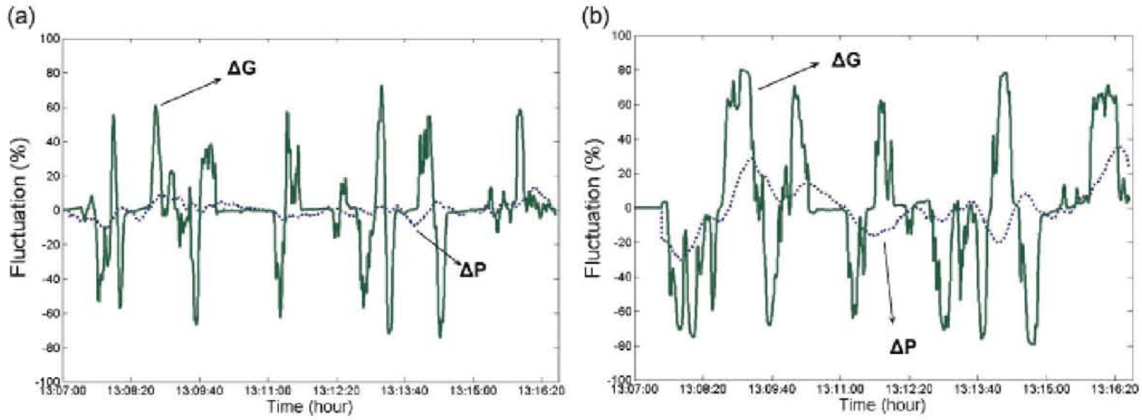

Figure 4. Irradiance fluctuation ΔG (solid green line) and power fluctuation ΔP (blue dashed line) evolution recorded at Milagro site during an almost 15-min period, for (a) $\Delta t = 10$ s; (b) $\Delta t = 60$ s

this work is restricted to $\Delta t < 600$ s, because this period of time represents a borderline in terms of grid operator reaction. Typically, below 600 s power fluctuations are absorbed by the grid as frequency fluctuations, thus affecting power quality. On the other hand, over 600 s the network operator can comfortably react by adding (or subtracting) power from other sources. In the range of $\Delta t < 600$ s frequency distributions of power fluctuations calculated by Equation (1) are very close to those given by Equation (2). This is clearly observed at Figure 5, which shows the distributions[1] of the maximum daily power fluctuation observed during a year (365 values, once per day), for Δt equal to 20 and 600 s. Therefore in this paper, the fluctuations have been calculated by Equation (1), in order to open the door to comparison with experiments performed at different sampling periods, like the ones referred above.

[1]Strictly speaking, a ***distribution*** is a curve corresponding to a ***continuous*** variable. In practice, fluctuation distributions are obtained as normalized histograms for a large number of fluctuation intervals of very narrow width, 1%.

4. IRRADIANCE FLUCTUATIONS

Figure 6 shows the irradiance fluctuations distributions observed at the Cintruenigo site during a full year (from May 2008 to April 2009) for $\Delta t = 10$, 20, 60, and 600 s. All the distributions are normalized, so that the total area below the curve equals one. Visual appearance gives a different impression because frequency axis has a logarithmic scale. These distributions are clearly symmetric, reflecting the

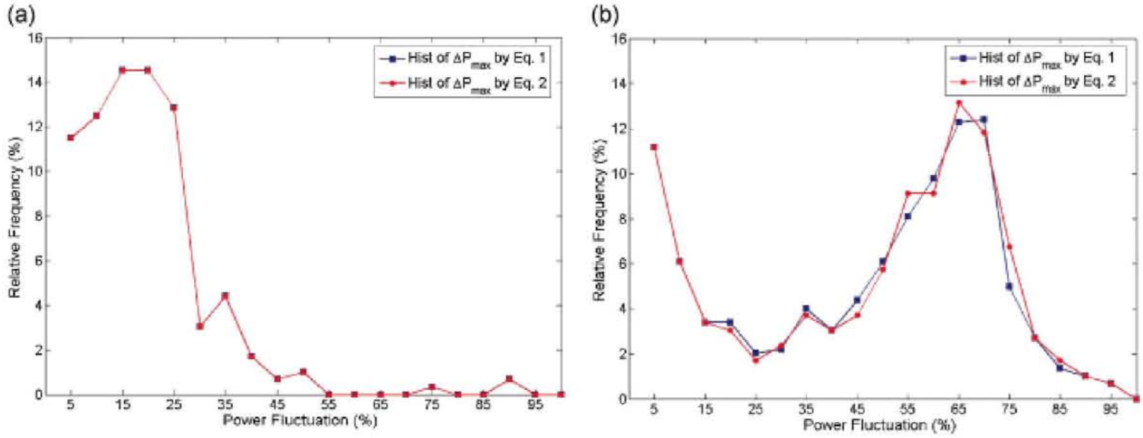

Figure 5. Distributions of the maximum daily power fluctuation, ΔP_{MAX}, observed during a year, for At equal to 20 s (a) and 600 s (b). The power fluctuation has been calculated in two ways, by Equation (1) (red line) and Equation (2) (blue line)

obvious fact that cloud passage entails, both, an irradiance reduction (when clouds arrive) and an irradiance increase (when clouds leave). A positive correlation between the fluctuation magnitude and the sampling time is observed again. Table II gathers the values of some fluctuation intervals. Note that a significant fluctuation let us say larger than 3% in 1 s, is relatively rare. In fact, this is why frequency is presented in logarithmic scale in Figure 6. However, the relative frequency is near 41% in 600 s.

Figure 7 shows the largest observed fluctuation versus Δt along the year. Values over 80% are observed for any $\Delta t > 2$ s. Values over 100% correspond to irradiances larger than 1000 W/m^2, which are typically associated to reflection effects caused by cloud edges. The 90th percentile has also been represented. It is about 20% below the largest fluctuation. It is noteworthy that all the irradiance fluctuation features calculated at the rest of places (and not presented here), essentially coincide with the features at Cintruénigo site, in accordance with the fact that all sites belong to the same climatic region. This way, the same mathematical description of the phenomenon applies for all the sites. In other words, the power fluctuations are not influenced by geographic aspects. Moreover, it has been checked that the monthly fluctuation distributions are very similar between them and also comparable to yearly distributions. In consequence, this represents an argument in favour of considering the fluctuations as a stationary statistic process. In other words, the distributions presented here can also be viewed as probability density functions, in yearly or monthly terms. However, stationarity is far from being preserved in daily terms. In fact, some days do exhibit frequent fluctuations while other days practically do not.

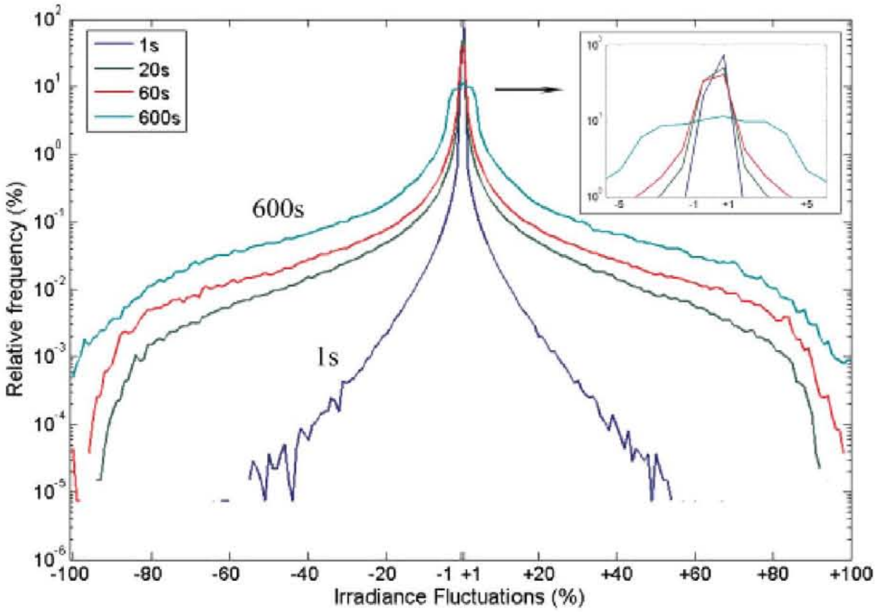

Figure 6. Distributions of the irradiance fluctuations, ΔG, registered at Cintruenigo site during a full year, for $\Delta t = 1$, 20, 60 and 600 s

Table II. Influence of Δt on the frequency distributions of the fluctuations

ΔG (%)	Δt (s)			
	1 s	20 s	60 s	600 s
$0\% \leq \Delta G \leq 3\%$	98.94%	92.51%	87.50%	59.37%
$3\% \leq \Delta G \leq 10\%$	0.92%	4.47%	7.61%	28.24%
$10\% \leq \Delta G \leq 50\%$	0.16%	2.71%	4.66%	11.25%
$50\% \leq \Delta G \leq 100\%$	2.35×10^{-4}%	0.32%	0.70%	1.35%

Grid operators require power fluctuation forecasts with similar anticipation weather forecasts; let us say in daily terms. Looking for that, we have analysed the fluctuations in these terms. Considering as relevant fluctuations those which absolute value is over a certain threshold, *i.e.* $\text{abs}(\Delta G_{\Delta t}) > u$, the total length of the day from sunrise to sunset, T_D, can be divided in two parts, $T_{\Delta G>u}$ and $T_{\Delta G \leq u}$, depending on the occurrence or not of such relevant fluctuations. As an example, Table III gives some values for $u = 3\%$ and $\Delta t = 20$ and 600 s, for 4 days. Figure 8 shows the frequency distribution of only relevant fluctuations for April 29th. These distribution functions can be adjusted to an exponential function:

$$f(x)|_{\Delta G>u} = ae^{-bx} \tag{3}$$

Obviously, the curve enclosed area must equal one. Hence, assuming $u << 100$ and considering that fluctuations larger than 100% are so scarce that can be neglected:

$$\int_u^{100} f(x)|_{\Delta G>u} \mathrm{d}x = \frac{a}{b}\left(e^{-bu} - e^{-b100}\right) \approx \frac{a}{b}e^{-bu} = 1$$

$$\Rightarrow a = be^{bu} \tag{4}$$

which leads to

$$f(x)|_{\Delta G>u} = be^{-b(x-u)} \tag{5}$$

Table III also presents b values calculated for the cases considered above. The corresponding regression coefficients, R^2, are close to one. It should be stressed that $T_{\Delta G>u}/T_D$ and b values are specific for each Δt and for each day, so they must be obtained from the analysis of the fluctuations observed on each particular day. Obviously, fluctuation

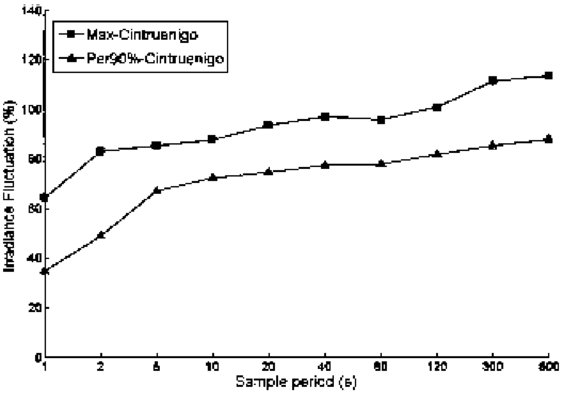

Figure 7. Maximum irradiance fluctuation ΔG and 90th percentile registered at Cintruenigo site

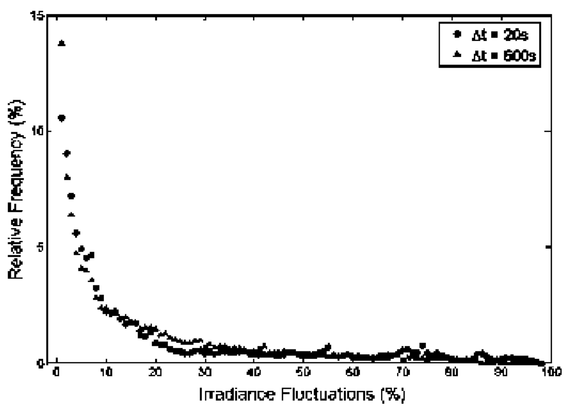

Figure 8. Frequency distribution of the irradiance fluctuations,

Table III. Distribution function parameters

Date	Kt	Δt (s)	$T_{\Delta G>u}/T_D$	b	R^2	ΔG_{max} (%)	$F(x > 40\%)$ (%)
1/May/2008	0.70	20 s	0.02	0.18	0.94	2	0.002
		600 s	0.27	0.68	0.90	25	0.007
8/Aug/2008	0.53	20 s	0.2	0.13	0.92	40	0.16
		600 s	0.67	0.09	0.89	82	2.35
2/Mar/2009	0.22	20 s	0.003	0.36	0.98	9	0.0
		600 s	0.36	0.21	0.97	30	0.01
29/Apr/2009	0.50	20 s	0.18	0.14	0.90	53	0.006
		600 s	0.70	0.09	0.92	97	0.02

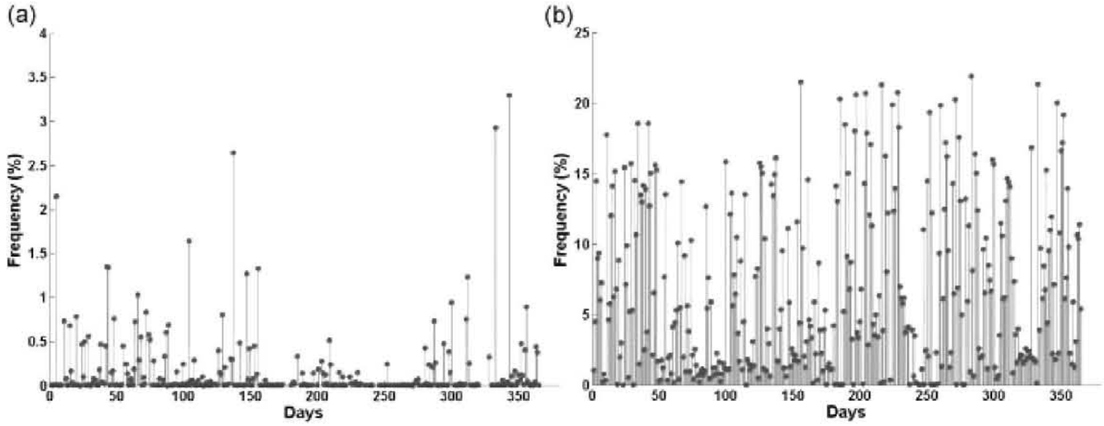

Figure 9. Evolution of the daily frequency of a irradiance fluctuation larger than 40% in Cintruenigo during a year (a) $\Delta t = 20$ s; (b) $\Delta t = 600$ s

occurrence increases when $T_{\Delta G>u}/T_D$ increases, and also when b decreases. The main benefit of this model is that it allows long data sequences (for example containing around 2520 numbers for $\Delta t = 20$ s) to be condensed into just two parameters, without any important loss of information. Moreover, the analytic character of the model allows easy calculations. For example, cumulative frequencies for any given fluctuation interval can easily be calculated now. Once a relevant fluctuation x happens, the cumulative frequency of being larger than y, is given by:

$$F(x > y)|_{\Delta G>u} = \int_{y}^{100} f(x)\mathrm{d}x = e^{-b(y-u)} \tag{6}$$

The frequency distribution Equation (7) and the absolute cumulative frequency Equation (8) are calculated multiplying this function by the frequency of having a relevant fluctuation. That is:

$$f(x) = \begin{cases} x < u; \& \left(1 - \frac{T_{\Delta G>u}}{T_D}\right)\frac{1}{u} \\ x > u; \& \frac{T_{\Delta G>u}}{T_D} b e^{-(x-u)} \end{cases} \tag{7}$$

$$F(x > y) = \frac{T_{\Delta G>u}}{T_D} F(x > y)|_{\Delta G>u} \tag{8}$$

Figure 9 presents the yearly evolution of this cumulative frequency for fluctuations larger than 40% for $\Delta t = 20$ and 600 s at Cintruénigo. It has been obtained by previous

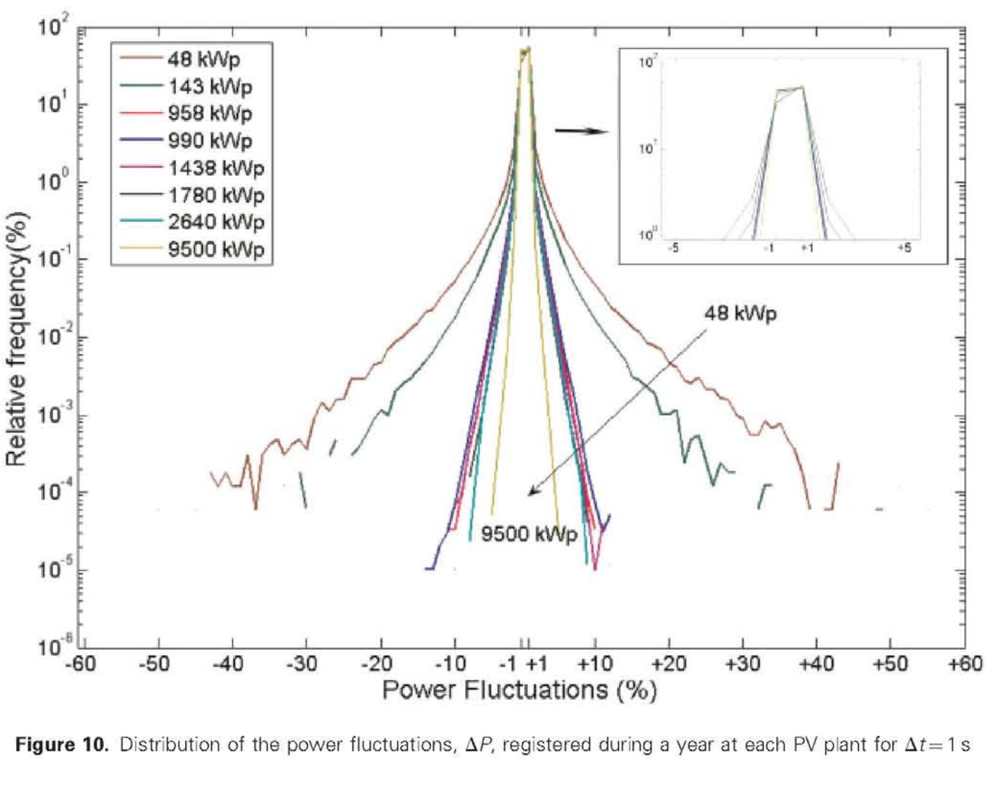

Figure 10. Distribution of the power fluctuations, ΔP, registered during a year at each PV plant for $\Delta t = 1$ s

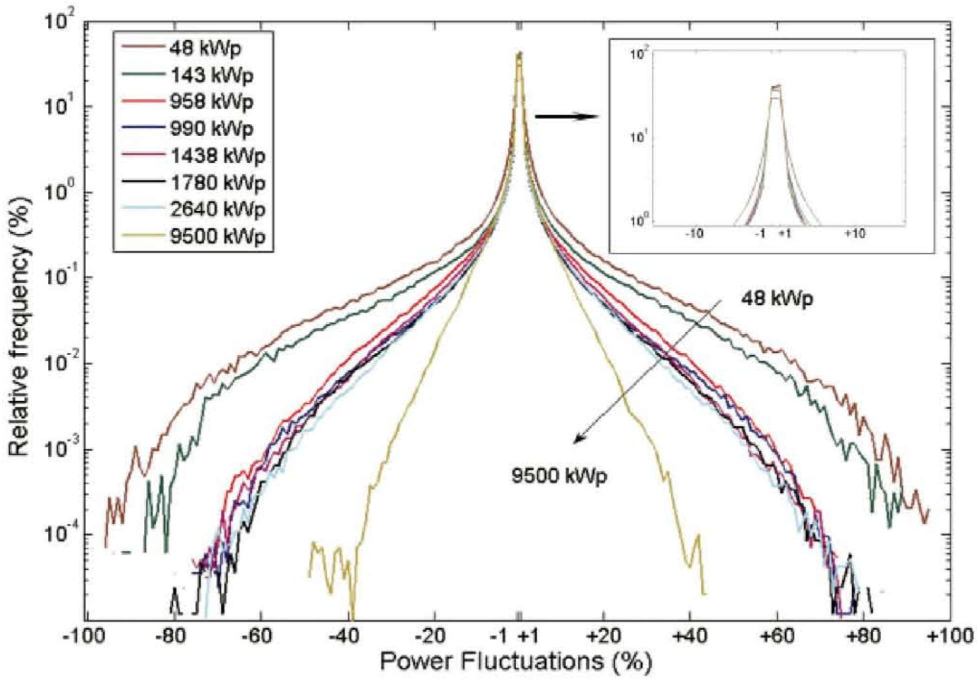

Figure 11. Distribution of the power fluctuations, ΔP, registered during a year at each PV plant for $\Delta t = 20$ s

calculation of a pair of ($T_{\Delta G>u}/T_D$) and b values for each day of the year. Interestingly enough, the occurrence of this fluctuation is concentrated in only a few days for small Δt. For example, for $\Delta t = 20$ s there are only 11 days where $F(x > 40\%)$ is above 1%. On the other hand, for $\Delta t = 600$ s, the number of days where $F(x > 40\%)$ is over 10% is 103. Currently ongoing and still provisional studies suggest that risky days result from the combination of high wind speed (about 60 km/h, or more) with intermediate daily clearness index ($0.35 < k_t < 0.65$). Because wind speed and clearness index can be predicted from 1 day to another (in fact, it is already being done in standard weather forecast), this

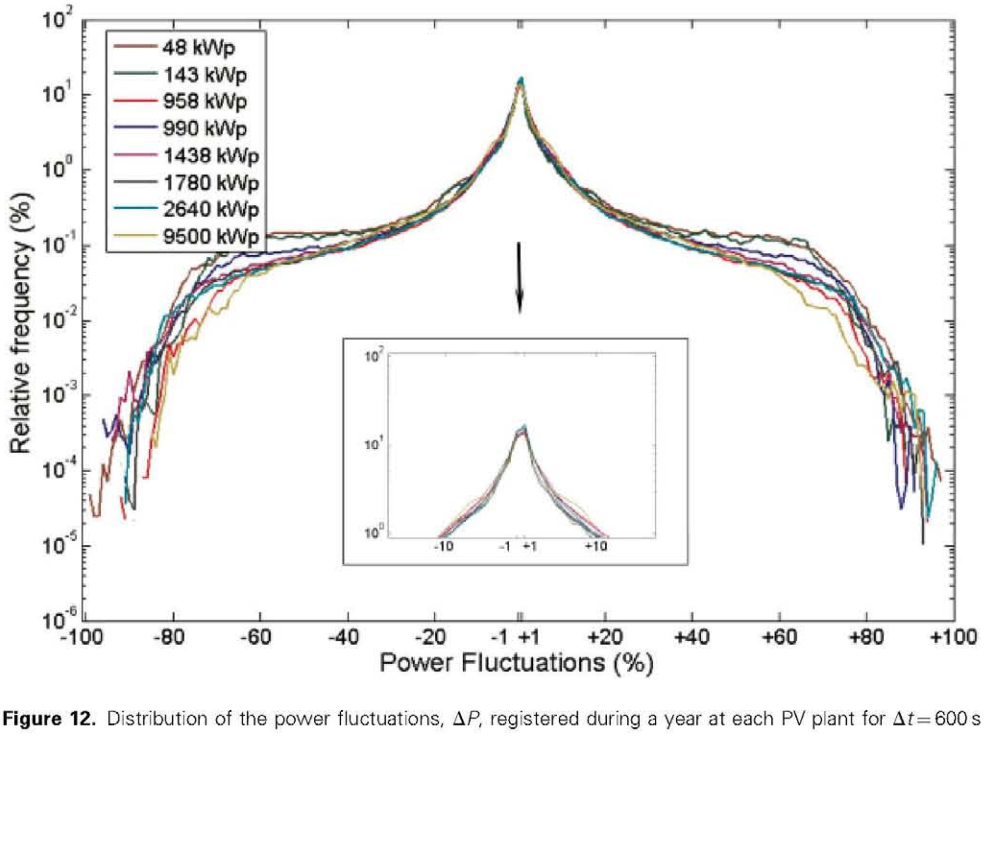

Figure 12. Distribution of the power fluctuations, ΔP, registered during a year at each PV plant for $\Delta t = 600$ s

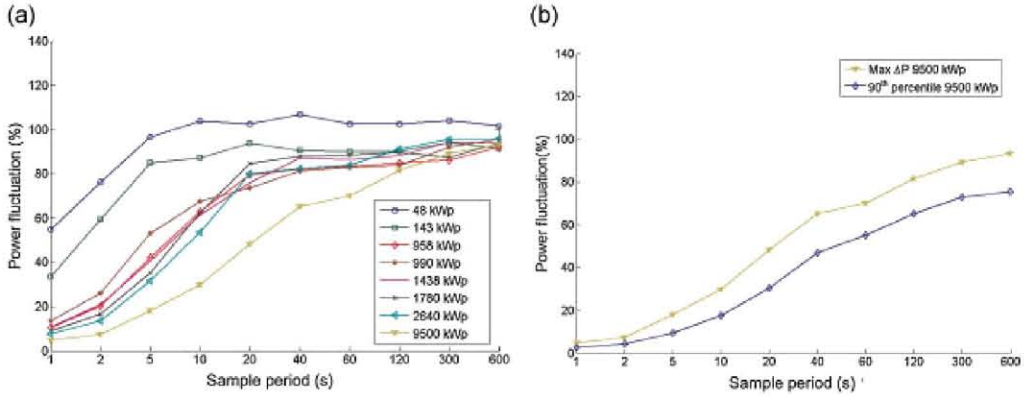

Figure 13. (a) Maximum power fluctuations, ΔP, registered during a year at each PV plant, (b) maximum power fluctuation, ΔP, and 90th percentile registered at Milagro site (9500 kWp) during a year

likely opens the door for future prediction of fluctuations in daily terms.

Finally, it must be mentioned that all the aforementioned irradiance fluctuation features at the Cintruénigo site described along this paper essentially coincide with all the other sites registered features, in coherence with the fact that all sites belong to the same climatic region.

5. POWER FLUCTUATIONS

Besides the intermittence of cloudiness, power output fluctuations are influenced by the size of the PV plant. *A priori*, the larger the PV plant is, the lower the power output fluctuation should be. In other words, it is anticipated that the PV plant size will smooth power output fluctuations. It is also straightforward to understand that the shorter the sampling time is, the more significant the smoothing effect should be. Figures 10, 11 and 12 show the power output fluctuation distributions observed along a full year (from May 2008 to April 2009) in all the here concerned PV plants, for $\Delta t = 1, 20$ and 600 s. As expected, the smoothing effect is more noticeable with size and is reduced with Δt.

Figure 13(a) shows for the full year, the largest fluctuation observed in the different PV plants versus Δt. Figure 13(b) shows the largest fluctuation and also the 90th percentile observed at Milagro (9.5 MWp) site. Once again, the smoothing effect increases with size and is reduced with Δt.

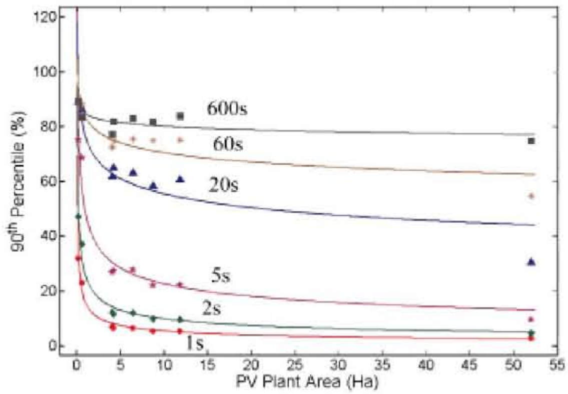

Figure 14. 90th percentile of the registered power fluctuations as a function of the PV plant area

Figure 14 shows the 90th percentile versus the PV plant size, with Δt as parameter. Table IV compiles the corresponding values. It is worth mentioning that they can be fitted to an exponential function, such as:

$$y = mx^n \tag{9}$$

Table IV. 90th percentile of the registered power fluctuations for each PV plant under study

PV plant	Peak power (kWp)	Area (Ha)	90th percentile (%)					
			1 s	2 s	5 s	20 s	60 s	600 s
Milagro section 1	48	0.21	32	47	75	89	90	89
Milagro section 2	143	0.63	23	37	69	86	88	84
Arguedas	958	4.1	7	12	28	64	75	84
Sesma	990	4.2	6	12	27	63	75	83
Cintruénigo	1438	6.4	6	11	27	61	75	83
Rada	1780	8.7	5	11	23	60	74	81
Castejón	2640	11. 8	5	10	22	58	72	81
Milagro	9500	52	3	4	10	30	54	74

Table V. Estimated m and n parameters

Δt	m	n	R^2
1 s	15.78	−0.49	0.98
2 s	25.71	−0.43	0.96
5 s	48.40	−0.33	0.93
20 s	76.38	−0.2	0.88
60 s	83.86	−0.08	0.82
600 s	85.20	−0.02	0.75

Table VI. Distribution function parameters for April 29th at Milagro (9.5 MWp) and Sesma (0.990 MWp) PV plants

PV plant	Milagro (9.5 MWp)		Sesma (0.990 MWp)	
Δt (s)	20 s	600 s	20 s	600 s
$T_{\Delta P>u}/T_D$	0.14	0.68	0.19	0.63
b	0.28	0.09	0.13	0.08
R^2	0.98	0.93	0.97	0.93

Table VII. Number of days during a year where cumulative frequency for power fluctuations larger than 40%, $F(x>40\%)$, is over 1 and 10%. Fluctuations have been calculated for $\Delta t = 20$, 600 s and for Milagro (9.5 MWp) and Sesma (0.990 MWp) PV plants.

PV plant	Milagro (9.5 MWp)				Sesma (0.990 MWp)			
Δt (s)	20 s		600 s		20 s		600 s	
$F(x>40\%)$	>1%	>10%	>1%	>10%	>1%	>10%	>1%	>10%
No. days	0	0	128	10	13	0	130	8

Table V presents the m and n values versus Δt. It is interesting to note that for $\Delta t = 1$ and 2 s, the n value is basically −0.5. Therefore, the smoothing effect for small Δt is accurately described by a $1/\sqrt{S}$ law, where S is the PV plant extension. This can be explained taking into consideration that shades typically move in one dimension while power is essentially related to surface or two dimensions. However, for the PV plant areas considered in this paper and for long $\Delta t(>20\,\text{s})$, the power fluctuations are not influenced by the size of the plant, due to the shadows have enough time to completely cover the plant.

The frequency distribution Equation (10) and the absolute cumulative frequency Equation (11) of relevant power fluctuations (abs($\Delta P_{\Delta t}$) > u) for a given day can be described similarly to the irradiance:

$$f(x) = \begin{cases} x < u; & \left(1 - \frac{T_{\Delta P>u}}{T_D}\right)\frac{1}{u} \\ x > u; & \frac{T_{\Delta P>u}}{T_D} b e^{-(x-u)} \end{cases} \quad (10)$$

and

$$F(x > y) = \frac{T_{\Delta P>u}}{T_D} F(x > y)|_{\Delta P>u} = \frac{T_{\Delta P>u}}{T_D} e^{-b(y-u)} \quad (11)$$

Now, the values of $(T_{\Delta P>u}/T_D)$ and b for each day depend on Δt and also on the PV plant size. Table VI presents some values for April 29th, u = 3%, $\Delta t = 20$ and 600 s, and for two different sites: Sesma (0.990 MWp) and Milagro (9.5 MWp). Table VII shows the number of days during a year where cumulative frequency for fluctuations larger than 40%, $F(x>40\%)$ is over 1 and 10%, for $\Delta t = 20$, 600 s and for Sesma and Milagro PV plants. The smoothing effect becomes evident in the lower frequencies of the biggest PV plant, but only for $\Delta t = 20$ s. Likewise, the occurrence of relevant fluctuations is concentrated on only a few days. Current studies are focused on the prediction of those problematic days through standard weather data. This will be critical to establish a relationship between parameter b and $T_{\Delta P>u}/T_D$ values depending on the PV plant size and the meteorological conditions of a particular day.

6. CONCLUSIONS AND OUTLOOK

Power supply quality and network security could be seriously affected by PV plants power fluctuations in a near future, due to irradiance variability. This work is based on 1 year data with a 1 s resolution from six different PV plants (adding up to 18 MWp). The analysis of the data has revealed the smoothing effect of PV plant size on power fluctuations. Moreover, such smoothing effect has been found strongly dependent on the sampling-time considered. An empirical expression has been proposed in order to calculate the fluctuation magnitude for short time periods.

The statistical study of the daily power fluctuations has allowed the analytic description of the fluctuation frequency, as well. Furthermore, current research efforts deal with the smoothing effect associated to the combination of the six PV plants and the forecast of the most risky days. Methods for daily prediction of wind speed and clearness index are well developed. In fact, this is routinely done in weather forecast. Hence, if it is finally confirmed, the relation between these meteorological parameters and power fluctuations will permit the prediction of the last ones. It is worth to note that the probability of a certain maximum power fluctuation is the key for establishing the maximum allowed PV penetration rate at a particular grid.

ACKNOWLEDGEMENTS

The authors would like to thank Red Eléctrica de España (REE) for their financial support and ACCIONA for authorizing measurements at its PV plants and for their staff helpful collaboration. Likewise, Pedro Zufiria has provided invaluable technical support on the analytic description of the fluctuation frequency. Finally, two anonymous reviewers have provided extremely clever comments to the first version of the paper. This work has been also supported by the Spanish Ministry of Education and Science (grant number: DPI2009-14713-C03-01).

REFERENCES

1. Beyer HG, Decker B, Luther J, Steinberg-Willms R. ''Spatial and temporal characteristics of short term fluctuations in solar radiation for PV-plant applications'', *10th European Photovoltaic Solar Energy Conference*, 8–12 April, 1991 Lisbon, Portugal, 453–456.
2. Otani K, Minowa J, Kurokawa K. Study on areal solar irradiance for analyzing areally-totalized PV systems. *Solar Energy Materials and Solar Cells* 1997; **47**: 281–288.
3. Woyte A, Thong VV, Belmans R, Nijs J. Voltage fluctuations on distribution level introduced by photovoltaic systems. *IEEE Transactions on Energy Conversion* 2006; **21**: 202–209.
4. Woyte A, Belmans R, Nijs J. Fluctuations in instantaneous clearness index: analysis and Statistics. *Solar Energy* 2007; **81**: 195–206.
5. Wiemken E, Beyer HG, Heydenreich W, Kiefer K. Power characteristics of PV ensembles: experiences from the combined power production of 100 Grid connected PV systems distributed over the area of Germany. *Solar Energy* 2001; **70**(6): 513–518.
6. Curtright E, Apt J. The character of power output from utility-scale photovoltaic systems. *Progress in Photovoltaic: Research and Applications* 2008; **16**: 241–247.
7. Murata A, Yamaguchi H, Otani K. A method of estimating the output fluctuation of many photovoltaic power generation systems dispersed in a wide area. *Electrical Engineering in Japan* 2009; **166**(4): 645–652.
8. Jewell WT, Ramakumar R. The effects of moving clouds on electric utilities with dispersed photovoltaic generation, Paper no 8 87 WM 229-8, presented at the *IEEE Power Engineering Society1987 Winter Meeting*, New Orleans, 1–6 February 1987.
9. Jewell WT, Ramakumar R, Hill SR. A Study of Dispersed Photovoltaic Generation on the PSO System. *IEEE Transactions on Energy Conversion* 1988; **3**(3).
10. Jewell WT, Unruh TD. Limits on cloud-induced fluctuation in photovoltaic generation. *IEEE Transactions on Energy Conversion* 1990; **5**(1): 8–14.
11. Chowdhury BH, Rahman S. Is central station photovoltaic power dispatchable? *IEEE Transactions on Energy Conversion* 1988; **3**(4): 747–754.
12. Chowdhury BH. Effect of central station photovoltaic plants on power system security, *Proceedings of 21st IEEE Photovoltaic Specialist Conference, Kissimmee*, FL, May 1990.
13. Chowdhury BH. Optimizing the integration of photovoltaic systems with electric utilities. *IEEE Transactions on Energy Conversion* 1992; **7**(1): 72–78.